RSC Advances

PAPER

View Article Online
View Journal | View Issue

Cite this: *RSC Adv.*, 2018, **8**, 17121

Heronamides G–L, polyene macrolactams from *Streptomyces niveus*†

Nan Ding,[a] Li Han,[a]* Yi Jiang,[b] Guiding Li,[b] Zehui Zheng,[a] Bixuan Cao,[a] Peipei Guan,[a] Yu Mu,[a] Bin Lin[c] and Xueshi Huang[a]*

Received 12th March 2018
Accepted 24th April 2018

DOI: 10.1039/c8ra02167h

rsc.li/rsc-advances

Six new polyene macrolactams, heronamides G–L (**1–6**), one new polyenoic acid derivative, niveamide B (**10**), together with four known compounds, BE-14106-6 (**7**), BE-14106 (**8**), GT32-B (**9**), and niveamide (**11**), were isolated from the fermentation broth of *Streptomyces niveus*. Their planar structures were elucidated by detailed analysis of spectroscopic data. The absolute configurations of compounds **1–6** were determined by calculated ECD spectra and analysis of the possible biosynthetic pathways. Compounds **1–6** and **8–11** did not exhibit any significant antimicrobial activities, cytotoxicities, or inhibitory effects on lipopolysaccharide-induced NO production in BV2 microglial cells.

Introduction

Polyene macrolactams refer to macrolactams possessing a 20- to 26-membered lactam ring with multiple double bonds in their scaffold.[1] Heronamides are a class of 20-membered polyene macrolactam with methyl groups at C-6, C-14, and an unsaturated hydrocarbon tail at C-19. Recent studies have proven that a thermal or photochemical cycloaddition is involved in the formation of heronamide derivatives.[1–3] Since the first heronamide, BE-14106, was reported in 1992,[4] only ten natural members including BE-14106,[4,5] GT32-B,[5] ML-449,[6] heronamides A–F,[7,8] and 8-deoxyheronamide C[9] had been isolated from actinomycetes and two derivatives of BE-14106 (BE-14106-6 and BE-14106-7) were semi-synthesized by O_2 and UV irradiation.[1] The heronamides exhibited a variety of biological activities, such as antiproliferative activity, weak antimicrobial activity, inhibitory activity against mixed lymphocyte reaction, and growth inhibition against fission yeast cells.[1,5,9]

In the process of our continuous study on new bioactive metabolites from actinomycetes, the chemical constituents of *Streptomyces niveus* (YIM 32862) isolated from forest soil collected from Great Khingan Mountains were investigated. Six new polyene macrolactams, heronamides G–L (**1–6**), and one new polyenoic acid derivative, niveamide B (**10**), together with four known compounds, BE-14106-6 (**7**), BE-14106 (**8**), GT32-B (**9**), and niveamide (**11**), were isolated from the ethyl acetate extract of the fermentation broth of *S. niveus*. These new compounds were elucidated by extensive interpretation of spectroscopic data. The absolute configurations of compounds **1–6** were determined by calculated ECD spectra and analysis of the possible biosynthetic pathways. The antimicrobial, cytotoxic activities, and inhibitory effects on lipopolysaccharide-induced NO production of **1–6** and **8–11** were evaluated. Herein, we report the fermentation, isolation, structure elucidation, biological activities evaluation, and possible biosynthetic pathways of these compounds.

Results and discussion

Fermentation broth (140 L) of *S. niveus* was collected and centrifuged to yield a clarified supernatant, then the supernatant was extracted by EtOAc. Chemical constituents in EtOAc extract were isolated by sequential chromatographies over Sephadex LH-20, silica gel, ODS, and semipreparative HPLC to obtain pure compounds heronamides **1–9** and niveamides **10** and **11** (Fig. 1).

From the proposed biosynthesis of heronamides in the literature,[3,6,7,10] the 9-hydroxy heronamide precursors were released from the PKS assembly; after that, transannular [6π + 4π] cycloaddition and S_N2-mediated ring formation following olefinic epoxidation occurred to construct different heronamides. Compared with that of known heronamides,[3,7] compounds **1–9** exhibited a similar biosynthetic relationship (Scheme 1).

Heronamide G (**1**) was obtained as an amorphous, colorless solid with a molecular formula of $C_{27}H_{37}NO_5$ (ten degrees of unsaturation) based on the HRESIMS peak at *m*/*z* 456.2758 $[M + H]^+$ and NMR data. Detailed analysis of ^1H NMR, ^{13}C NMR, and HSQC of **1** (Table 1) revealed it was almost identical to BE-

[a]*Institute of Microbial Pharmaceuticals, College of Life and Health Sciences, Northeastern University, Shenyang 110819, People's Republic of China. E-mail: hanli@mail.neu.edu.cn; huangxs@mail.neu.edu.cn*

[b]*Yunnan Institute of Microbiology, Yunnan University, Kunming 650091, People's Republic of China*

[c]*School of Pharmaceutical Engineering, Shenyang Pharmaceutical University, Shenyang 110016, People's Republic of China*

† Electronic supplementary information (ESI) available: 1D and 2D NMR, HRMS, and IR spectra for **1–6**, and **10**. See DOI: 10.1039/c8ra02167h

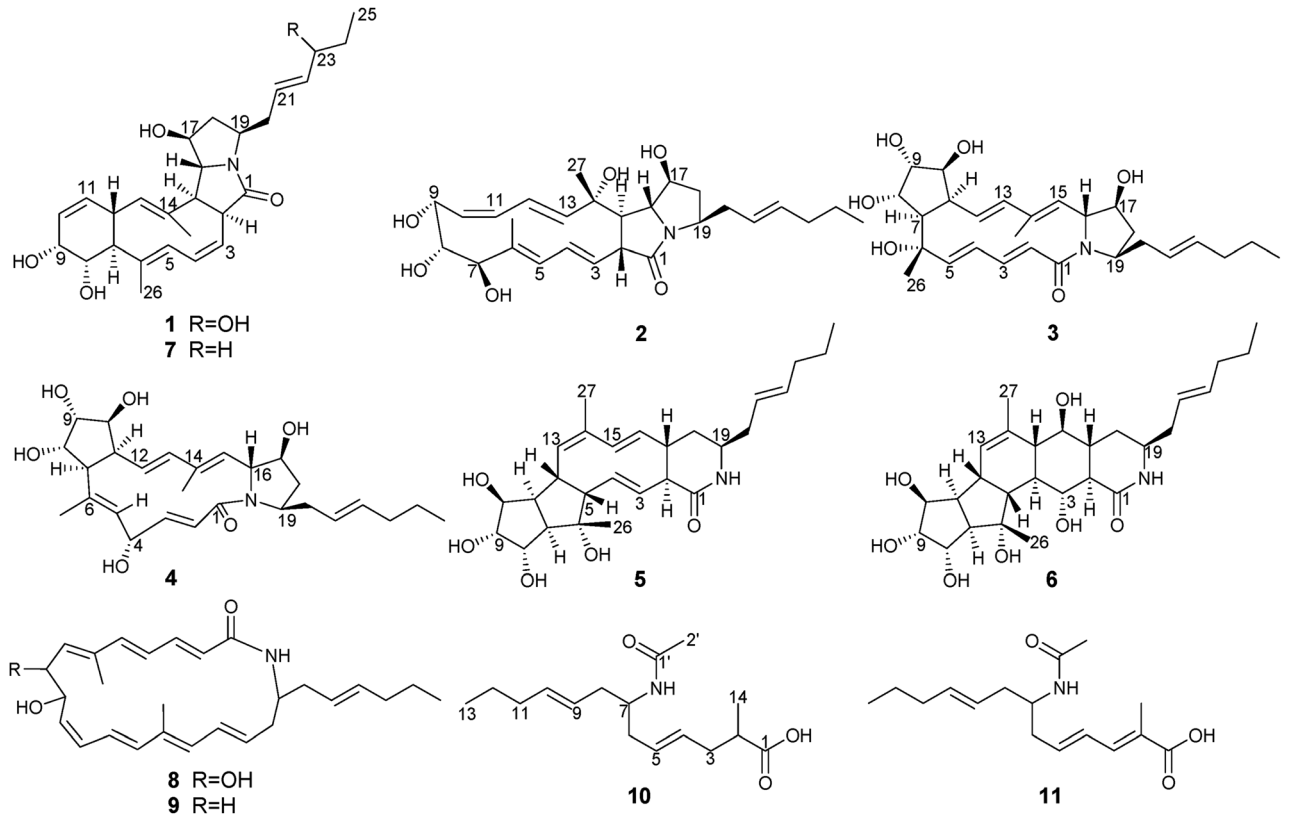

Fig. 1 Structures of compounds **1**–**11**.

14106-6 (**7**),[7] which was also isolated from the same strain BE-14106-6/nivelactam was first isolated from *S. niveus* (YIM 32860) by Li L. *et al.* and named as nivelactam.[11] BE-14106-6 was semi-synthesized from BE-14106 by O_2 induced conversion.[1] According to the same NMR data possessed by nivelactam and BE-14106-6, and the possible biosynthetic pathway in Scheme 1, the structure of BE-14106-6 was deemed reliable. The major difference between **1** and BE-14106-6 (**7**) is the presence of one more oxygenated methine signals ($\delta_{C/H}$ 71.6/3.80) and a hydroxy signal (δ_H 4.57) in **1** instead of a methylene signal in **7**. The COSY correlations of H-22 (δ_H 5.47)/H-23 (δ_H 3.80)/H-24 (δ_H 1.42) and HMBC correlations from 23-OH (δ_H 4.57) to C-22 (δ_C 136.6), C-23 (δ_C 71.6), and C-24 (δ_C 29.6) showed that the hydroxyl was located at C-23 (Fig. 2A). The similar ^{13}C NMR signals between **1** and **7** indicated they possessed the same relative configuration in the polyene macrolactam ring. Detailed analysis of ^1H–^1H coupling constants (Table 1) and NOE correlations (Fig. 2C) between H-2/H-5, H-13, H-15; H-7/H-13; H-15/H-13, H-17; H-4/H_3-26; H-8/H-9, H-12, H_3-26; H-12/H_3-27, and H-16/H_3-27 helped confirm the relative configuration of **1**. The *Z* configuration of double bond $\Delta^{3,4}$ was assigned by the $J_{3,4}$ values of 10.2 Hz. The *E* configurations of double bonds $\Delta^{5,6}$ and $\Delta^{13,14}$ were based on NOE correlations (Fig. 2C). The absolute configuration of **1** was determined by electronic circular dichroism (ECD) spectra with quantum chemical calculations using the time dependent density functional theory (TDDFT) method at the B3 LYP/6-311 ++ G(d) level. The experimental ECD spectrum of **1** matched the calculated spectrum of 2*S*,7*S*,8*S*,9*R*,12*R*,15*S*,16*R*,17*S*,19*R*-**1** (Fig. 2B). Hence, the structure of **1** was established and named as heronamide G.

Heronamide H (**2**) was purified as a white powder and assigned the molecular formula $C_{27}H_{39}NO_6$ (nine degrees of unsaturation) from the HRESIMS peak at *m*/*z* 474.2861 $[M + H]^+$. The ^1H NMR, ^{13}C NMR, and HSQC data of **2** (Table 1) showed the presence of two sp^2 nonprotonated carbons (δ_C 171.3 and 133.7), nine sp^2 methines ($\delta_{C/H}$ 141.1/5.42, 132.3/5.45, 130.9/4.94, 130.3/6.17, 129.6/5.97, 127.5/5.57, 126.4/5.48, 125.1/5.36, 124.9/5.76), one sp^3 oxygenated nonprotonated carbon (δ_C 71.2), eight sp^3 methines including four oxygenated ($\delta_{C/H}$ 78.9/3.38, 74.6/3.58, 73.6/3.79, and 65.0/3.89) and four other methines ($\delta_{C/H}$ 66.4/3.53, 57.1/2.05, 53.2/3.28, and 51.6/3.72), four methylenes ($\delta_{C/H}$ 39.3/2.31, 1.67; 36.6/2.34, 2.17; 33.5/1.96; and 21.4/1.35), and three methyls ($\delta_{C/H}$ 19.2/1.29, 12.9/0.87, and 10.8/1.66). In addition to an amide carbonyl and five double bonds accounting for six degrees of unsaturation, **2** was required to be a tricyclic skeleton according to its unsaturation. Careful interpretation of ^1H–^1H COSY of **2** revealed the presence of two substructures (subunits A and B) (Fig. 3A). HMBC correlations from H-2 (δ_H 3.28), H-3 (δ_H 4.94), H-19 (δ_H 3.72) to C-1 (δ_C 171.3) indicating the location of the amide carbonyl, from H_3-26 (δ_H 1.66) to C-5 (δ_C 127.5), C-6 (δ_C 133.7), and C-7 (δ_C 78.9) and from H_3-27 (δ_H 1.29) to C-13 (δ_C 141.1), C-14 (δ_C 71.2), and C-15 (δ_C 57.1) completing the connections between

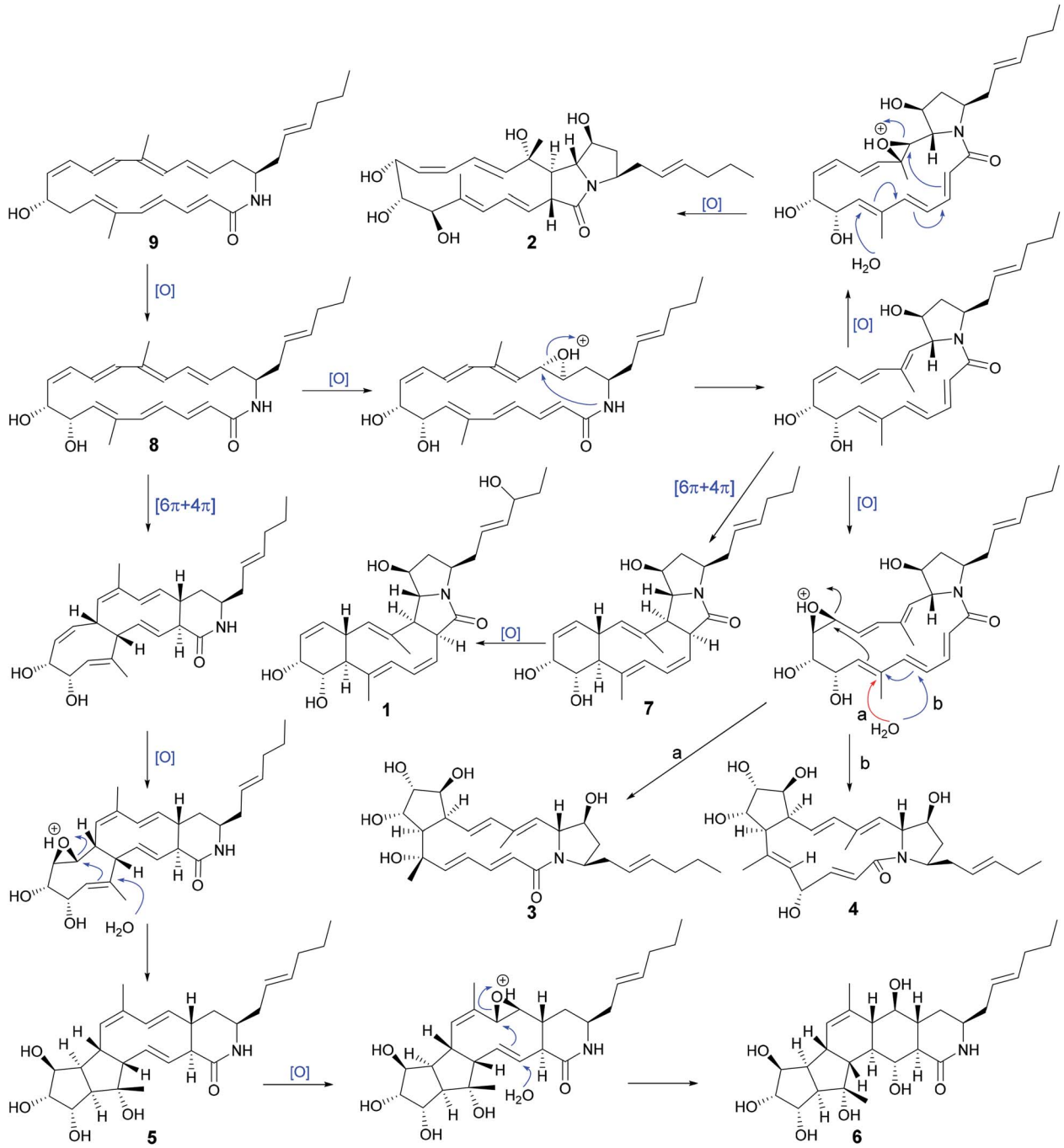

Scheme 1 Possible biosynthetic pathways between compounds **1**–**9**.

subunits A and B, helped establish the gross structure of **2** (Fig. 3A).

A detailed NOESY analysis of **2** between H-2/H-4, H-16; H_3-26/H-4, H-8, H-9; H-9/H-12, and H_3-27/H-12, H-16 determined the H-2, H-4, 6-CH_3, H-8, H-9, H-12, 14-CH_3, H-16 were placed on the same face of the ring system, while the correlations between H-3/H-5, H-15; H-5/H-7; H-11/H-10, H-13; H-15/H-13, H-17, and H-16/H-20 revealed the H-3, H-5, H-7, H-10, H-11, H-13, H-15, H-17, H-19 were on the opposite side (Fig. 3C). Compared to **1**, the difference of relative configurations of H-2 and H-15 was further supported by the $J_{\text{H-2/H-15}} = 12.8$ Hz in **2** instead of $J_{\text{H-2/H-15}} = 9.1$ Hz in **1**. Analysis of the possible biosynthetic pathways of **1** and **2** indicated the two compounds were completely different in the formation of the five-membered lactam ring (Scheme 1), which further explained the different relative configuration of H-2/H-15 between **1** and **2**. The ^{1}H–^{1}H coupling constants and NOE correlations (Fig. 3C) also helped establish the configuration of double bonds in **2**: *E* $\Delta^{3,4}$ ($J_{3,4}$ 14.9 Hz), *E* $\Delta^{5,6}$ (NOE correlations between H-3/H-5, H_3-26/H-4), *Z* $\Delta^{10,11}$ ($J_{10,11}$ 11.0 Hz), and *E* $\Delta^{12,13}$ ($J_{12,13}$ 15.6 Hz). The

Table 1 ^{1}H NMR (600 MHz) and ^{13}C NMR (150 MHz) data for compounds **1–4** in DMSO-d_6

	1		**2**		**3**		**4**	
No.	δ_C, type	δ_H, mult (J in Hz)	δ_C, type	δ_H, mult (J in Hz)	δ_C, type	δ_H, mult (J in Hz)	δ_C, type	δ_H, mult (J in Hz)
1	173.7, C		171.3, C		167.1, C		166.3, C	
2	53.1, CH	3.47, ddd (9.1, 6.8, 2.0)	53.2, CH	3.28, dd (12.8, 10.0)	129.5, CH	5.85, d (15.6)	124.1, CH	5.56, d (15.5)
3	124.6, CH	5.36, dd (10.2, 6.8)	130.9, CH	4.94, dd (14.9, 10.0)	137.4, CH	6.42, dd (15.6, 10.4)	143.9, CH	6.14, d (15.5, 8.3)
4	131.2, CH	6.60, ddd (10.2, 9.7, 2.0)	130.3, CH	6.17, dd (14.9, 11.0)	127.6, CH	5.92, dd (15.7, 10.4)	68.3, CH	4.61, m
5	128.4, CH	5.37, d (9.7)	127.5, CH	5.57, dd (11.0, 1.1)	144.0, CH	5.58, d (15.7)	130.2, CH	4.84, d (9.4)
6	131.7, C		133.7, C		74.1, C		136.8, C	
7	51.8, CH	1.95, t (10.5)	78.9, CH	3.38, brd (8.4)	51.2, CH	1.95, dd (12.3, 7.9)	60.6, CH	2.59, dd (12.1, 8.2)
8	68.5, CH	3.67, ddd (10.5, 7.8, 4.1)	74.6, CH	3.58, brd (8.4)	74.7, CH	4.29, m	73.8, CH	4.13, m
9	65.2, CH	3.97, ddd (4.9, 4.1, 3.7)	65.0, CH	3.89, brd (9.5)	75.9, CH	3.65, m	78.1, CH	3.68, m
10	127.9, CH	5.77, m[a]	126.4, CH	5.48, dd (11.0, 9.5)	77.4, CH	3.60, brd (3.6)	75.2, CH	3.77, m
11	130.8, CH	5.76, m[a]	129.6, CH	5.97, t (11.0)	45.7, CH	2.97, td (10.8, 4.6)	48.0, CH	3.05, ddd (12.1, 8.6, 5.2)
12	41.5, CH	2.72, t (11.0)	124.9, CH	5.76, dd (15.6, 11.0)	125.5, CH	5.64, dd (15.6, 10.8)	125.4, CH	5.68, dd (16.1, 8.8)
13	130.6, CH	4.95, d (11.0)	141.1, CH	5.42, d (15.6)	138.0, CH	5.89, d (15.6)	136.3, CH	5.63, d (16.1)
14	135.9, C		71.2, C		136.3, C		135.0, C	
15	56.3, CH	3.13, t (9.1)	57.1, CH	2.05, dd (12.8, 9.0)	129.6, CH	4.81, d (10.0)	131.7, CH	4.84, d (9.2)
16	65.9, CH	3.74, m[a]	66.4, CH	3.53, dd (9.0, 6.7)	65.9, CH	4.29, dd (9.8, 2.7)	65.6, CH	4.34, dd (9.2, 3.1)
17	73.7, CH	3.74, m	73.6, CH	3.79, m	75.8, CH	3.92,m	76.2, CH	3.89, m
18	40.7, CH_2	2.30, m	39.3, CH_2	2.31, m	35.4, CH_2	1.98, m	35.4, CH2	1.99, m
		1.67, m		1.67, m		1.68, m		1.67, ddd (12.8, 4.6, 4.6)
19	50.9, CH	3.75, m	51.6, CH	3.72, m	56.9, CH	3.98, m	57.0, CH	4.02, m
20	35.9, CH_2	2.37, dt (13.7, 7.3)	36.6, CH_2	2.34, m	36.8, CH_2	2.51, m	36.7, CH2	2.50, m
		2.25, m		2.17, m		2.34, m		2.32, m
21	123.9, CH	5.48, m	125.1, CH	5.36, m	127.4, CH	5.35, m	127.3, CH	5.34, m
22	136.6, CH	5.47, m	132.3, CH	5.45, m	132.9, CH	5.42, m	132.9, CH	5.41, m
23	71.6, CH	3.80, m	33.5, CH_2	1.96, q (7.0)	34.7, CH_2	1.96, q (7.3)	34.7, CH2	1.95, q (7.3)
24	29.6, CH_2	1.42, m	21.4, CH_2	1.35, sxt (7.0)	22.6, CH_2	1.35, sxt (7.3)	22.6, CH2	1.34, sxt (7.3)
		1.38, m						
25	9.2, CH_3	0.83, t (7.4)	12.9, CH_3	0.87, t (6.1)	14.0, CH_3	0.87, t (7.4)	14.0, CH3	0.86, t (7.3)
26	11.8, CH_3	1.65, s	10.8, CH_3	1.66, s	22.7, CH_3	1.25, s	15.1, CH3	1.44, s
27	15.7, CH_3	1.29, s	19.2, CH_3	1.29, s	14.0, CH_3	1.83, s	12.9, CH3	1.71, s
6-OH						4.75, s		4.88, d (4.3)
7-OH				4.74, brs				
8-OH		4.26, d (7.8)		4.73, brs		4.33, brs		4.25, brs
9-OH		4.65, d (4.9)		4.45, d (5.1)		4.52, d (3.1)		4.62, brs
10-OH						4.79, d (3.7)		4.99, brs
14-OH				4.67, brs				
17-OH		5.11, d (4.7)		5.67, brs		5.28, d (3.8)		5.33, d (6.4)
23-OH		4.57, d (4.5)						

[a] Overlapping signals.

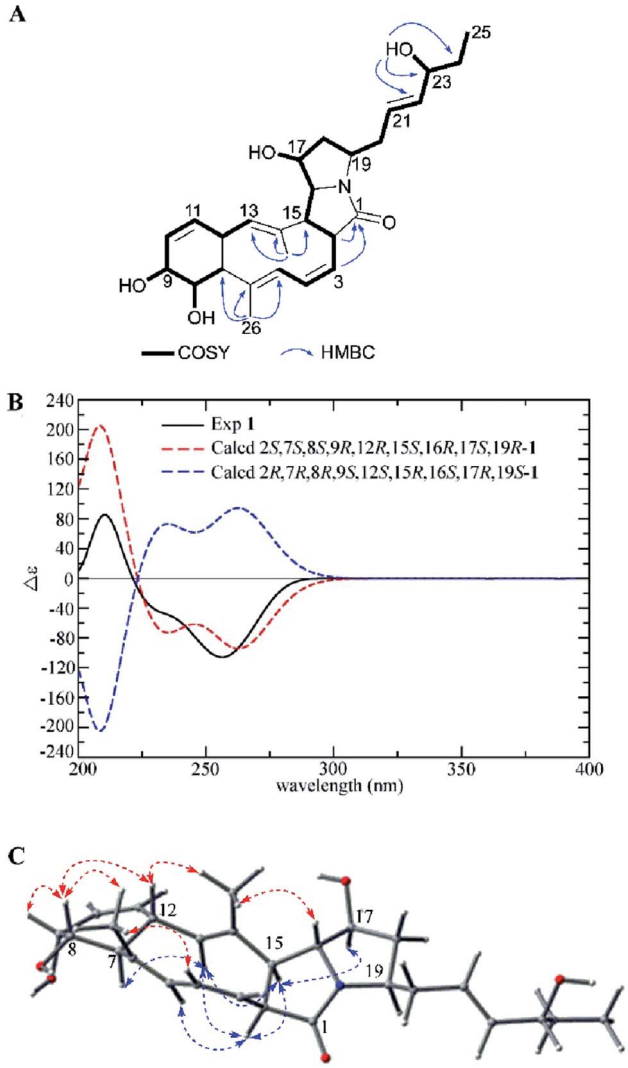

Fig. 2 (A) COSY and key HMBC correlations of **1**, (B) comparison of the experimental ECD spectra of **1** with the calculated ECD spectra, and (C) key NOEs observed in **1**.

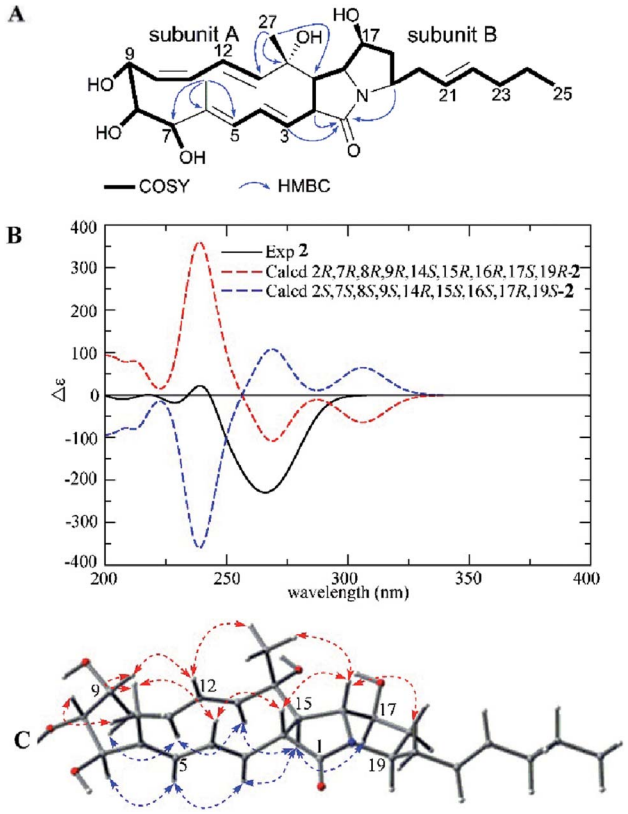

Fig. 3 (A) COSY and key HMBC correlations of **2**, (B) comparison of the experimental ECD spectra of **2** with the calculated ECD spectra, and (C) key NOEs observed in **2**.

experimental ECD spectrum of **2** showed the same pattern as the calculated ECD spectrum 2*R*,7*R*,8*R*,9*R*,14*S*,15*R*,16*R*,17*S*,19*R*-**2** (Fig. 3B). Hence, the absolute configuration of **2** was determined as shown.

Compound **3** was isolated as a white powder. The molecular formula of **3** was determined to be $C_{27}H_{39}NO_6$ (nine degrees of unsaturation) based on the HRESIMS peak at *m*/*z* 474.2870 $[M + H]^+$. The ^1H NMR, ^{13}C NMR, and HSQC spectra revealed the presence of one amide carbonyl (δ_C 167.1), one nonprotonated olefinic carbon (δ_C 136.3), and nine olefinic methines ($\delta_{C/H}$ 144.0/5.58, 138.0/5.89, 137.4/6.42, 132.9/5.42, 129.6/4.81, 129.5/5.85, 127.6/5.92, 127.4/5.35, and 125.5/5.64), explaining six degrees of unsaturation. Hence, **3** should be a tricyclic structure. Detailed analysis of the ^1H–^1H COSY correlations showed the presence of three substructures (C-2 to C-5, C-7 to C-13, and C-15 to C-25) (Fig. 4A). In addition, the HMBC correlations from H-2 (δ_H 5.85), H-3 (δ_H 6.42) to C-1 (δ_C 167.1), from H_3-26 (δ_H 1.25) to C-5 (δ_C 144.0), C-6 (δ_C 74.1), C-7 (δ_C 51.2), from H-9 (δ_H 3.65) to C-7 (δ_C 51.2), C-10 (δ_C 77.4), C-11 (δ_C 45.7), and from H_3-27 (δ_H 1.83) to C-13 (δ_C 138.0), C-14 (δ_C 136.3), C-15 (δ_C 129.6) connected three subunits in **3** (Fig. 4A).

The relative configuration of **3** was deduced by careful interpretation of the NOE correlations and coupling constants (Table 1). NOE cross peaks observed between H-2/H-4, H-16, H_3-27; H_3-26/H-4, H-8, H-12; H-8/H-9 and H_3-27/H-12, H-16 demonstrated that the H-2, H-4, 6-CH_3, H-8, H-9, H-12, 14-CH_3, and H-16 were located on the same side, while the NOE cross peaks between H-5/H-3, H-7; H-11/H-7, H-10, H-13 and H-15/H-13, H-17; H-17/H-19 indicated that H-3, H-5, H-7, H-10, H-11, H-13, H-15, H-17, H-19 were on the other side (Fig. 4C). The large $^3J_{HH}$ values of double bonds $\Delta^{2,3}$ ($J_{2,3}$ 15.6 Hz), $\Delta^{4,5}$ ($J_{4,5}$ 15.7 Hz), and $\Delta^{12,13}$ ($J_{12,13}$ 15.6 Hz) together with the NOE correlations between H_3-27/H-12, H-15/H-13 revealed the *E* configurations of the four double bonds in the macrolactam ring in **3**. The experimental ECD spectrum of **3** was similar to the calculated ECD curve of 6*S*,7*R*,8*S*,9*R*,10*S*,11*S*,16*R*,17*S*,19*R*-**3** (Fig. 4B). Therefore, the structure of **3** was established and named as heronamide I.

Heronamide J (**4**) was obtained as a white powder. The molecular formula of **4** was established as $C_{27}H_{39}NO_6$ on the basis of HRESIMS at *m*/*z* 474.2869 $[M + H]^+$, indicating nine degrees of unsaturation. The ^1H and ^{13}C NMR data of **4** were very similar to those of **3** except for the presence of an oxygenated methine ($\delta_{C/H}$ 68.3/4.61) and a nonprotonated olefinic

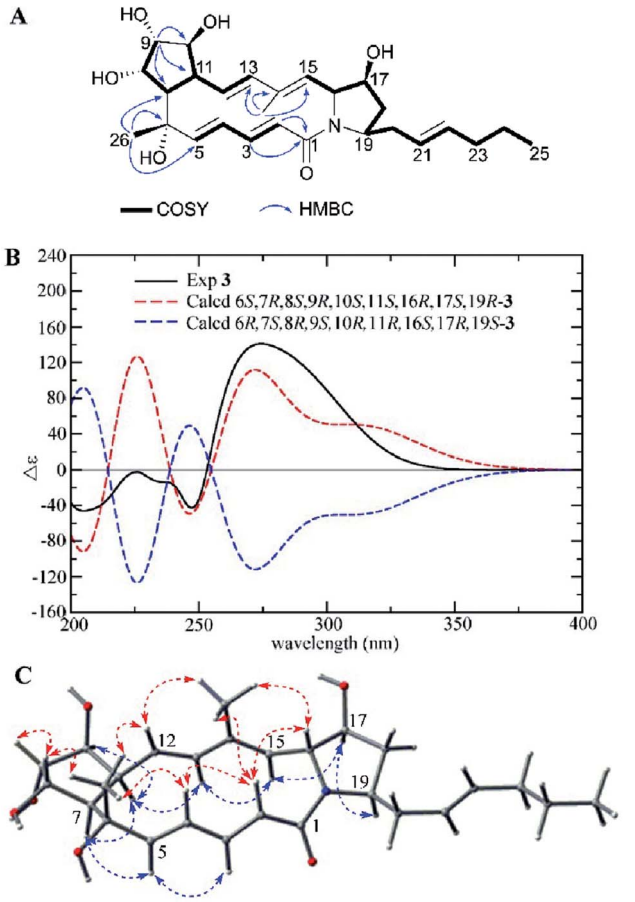

Fig. 4 (A) COSY and key HMBC correlations of **3**, (B) comparison of the experimental ECD spectra of **3** with the calculated ECD spectra, and (C) key NOEs observed in **3**.

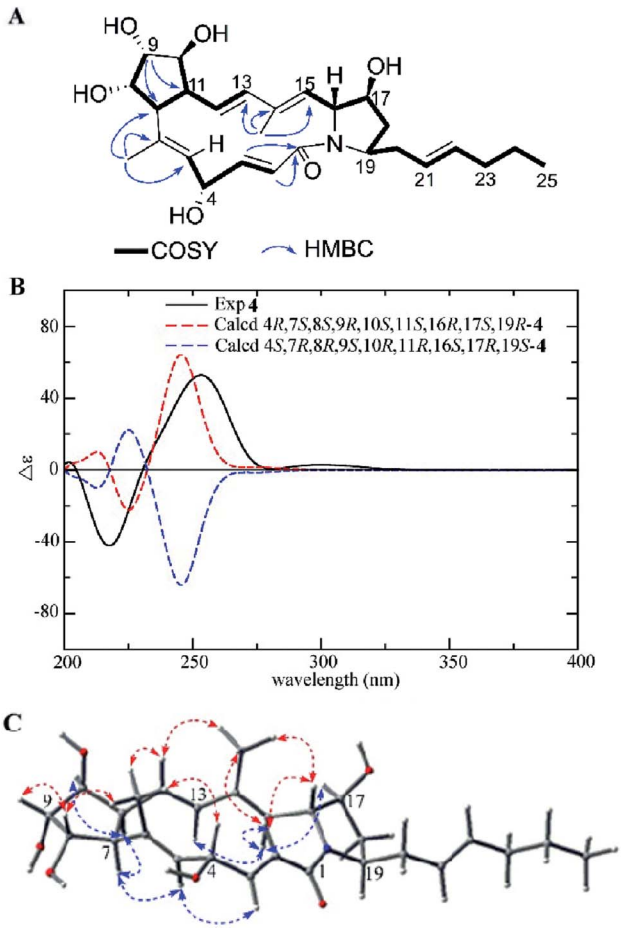

Fig. 5 (A) COSY and key HMBC correlations of **4**, (B) comparison of the experimental ECD spectra of **4** with the calculated ECD spectra, and (C) key NOEs observed in **4**.

carbon (δ_C 136.8) instead of an oxygenated quaternary carbon and an olefinic methine in **3**. Interpretation of ^{1}H–^{1}H COSY correlations from H-2 to H-5 indicated the double bond at C-4/C-5 in **3** translocated to C-5/C-6 in **4** and the hydroxyl located at C-4 in **4**. The HMBC correlations from H_3-26 (δ_H 1.44) to C-5 (δ_C 130.2), C-6 (δ_C 136.8), and C-7 (δ_C 60.6) further confirmed the speculative structure of **4** (Fig. 5A). The relative configuration of **4** was determined by NOE correlations and coupling constants (Table 1). NOE interactions observed between H_3-26/H-4, H-8; H-8/H-9, and H_3-27/H-12, H-16 revealed H-4, 6-CH_3, H-8, H-9, H-12, 14-CH_3, and H-16 were located on the same side, and NOE correlations between H-5/H-7; H-11/H-7, H-10, and H-15/H-13, H-17 along with a comparison of ^{13}C NMR with **3** presented H-5, H-7, H-10, H-11, H-13, H-15, H-17, and H-19 on the opposite (Fig. 5C). The *E* configurations of the double bonds in the macrolactam ring were assigned by the coupling constants $\Delta^{2,3}$ ($J_{2,3}$ 15.5 Hz), $\Delta^{12,13}$ ($J_{12,13}$ 16.1 Hz) and the NOE correlations (Fig. 5C). The experimental ECD was almost identical to the calculated ECD curve of 4*R*,7*S*,8*S*,9*R*,10*S*,11*S*,16*R*,17*S*,19*R*-**4** (Fig. 5B). On the basis of the foregoing evidence, the structure of **4** was determined.

Compound **5** was isolated as a white powder with a molecular formula of $C_{27}H_{39}NO_5$ (nine degrees of unsaturation) as shown by the HRESIMS peak at *m*/*z* 458.2912 $[M + H]^+$. The ^{13}C NMR data (Table 2) indicated the presence of an amide carbonyl (δ_C 171.8) and eight sp^2 olefinic carbons (δ_C 126.4 to 139.6), accounting for five degrees of unsaturation. Thus, there was a tetracyclic skeleton in **5**. A close inspection of the ^{1}H–^{1}H COSY correlations disclosed three substructures A, B, and C (Fig. 6A). The multiple HMBC correlation signals from NH (δ_H 7.50) to C-1 (δ_C 171.8) and C-2 (δ_C 55.7), from H-16 (δ_H 4.93) to C-18 (δ_C 30.0) indicated the connection between subunit A, subunit B and the position of amide carbonyl; from H_3-26 (δ_H 1.08) to C-5 (δ_C 62.0), C-6 (δ_C 79.5) and C-7 (δ_C 60.6), from H-12 (δ_H 2.92) to C-6 (δ_C 79.5), C-10 (δ_C 74.7) and C-11 (δ_C 51.3) revealed the connection of subunits B and C; while H-7 (δ_H 2.24) to C-9 (δ_C 79.5) suggested C-8 was linked to C-9; and H_3-27 (δ_H 1.74) to C-13 (δ_C 134.3), C-14 (δ_C 130.8), C-15 (δ_C 139.6) showed C-14 was substituted by a methyl, and confirmed the gross structure of **5**.

The relative configuration of **5** was determined by detailed analysis of a NOESY experiment. NOE correlations between H-3/H-5, H-17; H-5/H_3-26, H-8; H-8/H_3-26, H-9 and H-15/H-12, H-17 positioned H-3, H-5, 6-CH_3, H-8, H-9, H-12, H-15, and H-17 on the same side of the ring system, while the NOE cross peaks between H-2/H-4, H-16, H-19; H-4/6-OH; H-11/H-10, H-13 and

Table 2 ^{1}H NMR (600 MHz) and ^{13}C NMR (150 MHz) data for compounds **5** and **6** and **10** in DMSO-d_6

	5		**6**		**10**	
No.	δ_C, type	δ_H, mult (J in Hz)	δ_C, type	δ_H, mult (J in Hz)	δ_C, type	δ_H, mult (J in Hz)
1	171.8, C		175.1, C		176.6, C	
2	55.7, CH	2.17, t (9.1)	47.8, CH	1.83, m[a]	38.7, CH	2.31, m
3	127.5, CH	4.99, dd (15.9, 9.1)	74.6, CH	3.39, t (9.8)	35.7, CH_2	2.23, m
						2.02, m
4	139.5, CH	4.65, dd (15.9, 10.2)	42.9, CH	1.34, m	128.7, CH	5.36, m
5	62.0, CH	2.40, dd (10.2, 8.2)	52.7, CH	1.91, dd (8.5, 5.2)	127.9, CH	5.36, m
6	79.5, C		81.3, C		36.2, CH_2	1.98, m
7	60.6, CH	2.24, dd (9.7, 7.6)	61.5, CH	2.10, dd (9.5, 6.3)	47.8, CH	3.67, m
8	74.6, CH	3.64, ddd (7.6, 6.4, 4.3)	73.9, CH	3.58, q (5.9)	36.2, CH_2	2.06, m
9	79.5, CH	3.56, ddd (4.3, 3.4, 3.1)	78.9, CH	3.49, q (4.1)	126.2, CH	5.32, m
10	74.7, CH	3.78, ddd (6.8, 4.2, 3.1)	75.3, CH	3.82, dt (6.9, 4.3)	131.4, CH	5.40, m
11	51.3, CH	2.59, t (8.9)	48.9, CH	2.43, ddd (9.2, 7.2, 1.9)	33.5, CH_2	1.92, m
12	42.8, CH	2.92, t (7.4)	37.4, CH	2.50, m[a]	21.5, CH_2	1.32, m
13	134.3, CH	5.24, d (6.8)	133.1, CH	5.39, brs	12.8, CH_3	0.85, t (7.3)
14	130.8, C		136.7, C		15.8, CH_3	1.01, d (6.8)
15	139.6, CH	5.69, d (16.4)	48.4, CH	1.72, t (10.7)		
16	126.4, CH	4.93, dd (16.4, 8.4)	72.3, CH	3.18, q (9.3)		
17	40.5, CH	2.01, m	38.3, CH	1.52, m		
18	30.0, CH_2	2.04, m	27.7, CH_2	2.17, m		
		1.84, m		1.44, m		
19	50.0, CH	3.37, m	50.3, CH	3.36, m		
20	39.7, CH_2	2.23, m	39.2, CH_2	2.17, m		
		2.14, m		2.07, m		
21	127.0, CH	5.38, m	126.6, CH	5.35, m		
22	133.3, CH	5.47, m	133.7, CH	5.48, m		
23	34.6, CH	1.96, q (7.3)	34.7, CH_2	1.95, q (7.2)		
24	22.5, CH_2	1.34, sxt (7.3)	22.5, CH_2	1.34, sxt (7.2)		
25	14.0, CH_3	0.85, t (7.4)	14.0, CH_3	0.86, t (7.4)		
26	23.3, CH_3	1.08, s	24.0, CH_3	1.15, s		
27	20.1, CH_3	1.74, s	20.3, CH_3	1.82, s		
1′					167.8, C	
2′					22.1, CH_3	1.76, s
–NH		7.50, d (2.5)		7.92, d (1.7)		7.57, d (8.5)
–COOH						12.11, brs
3-OH				6.51, s		
6-OH		3.79, s		2.70, s		
8-OH		4.18, d (6.4)		4.12, d (5.9)		
9-OH		4.36, d (3.4)		4.36, d (4.1)		
10-OH		4.70, d (4.2)		4.69, d (4.3)		
16-OH				4.59, d (8.1)		

[a] Overlapping signals.

H_3-27/H-13, H-16 demonstrated H-2, H-4, 6-OH, H-7, H-10, H-11, H-13, 14-CH_3, H-16, and H-19 were on the other face of the ring system (Fig. 6C).

The E configurations of double bonds $\Delta^{3,4}$, $\Delta^{15,16}$, and Z configuration of double bond $\Delta^{13,14}$ were established according to the $J_{3,4}$ values (15.9 Hz), $J_{3,4}$ values (16.4 Hz), and the NOE correlations between H_3-27/H-13, respectively. The experimental ECD spectrum of **5** was conformed to the calculated ECD curve of 2*S*,5*S*,6*S*,7*R*,8*S*,9*S*,10*S*,11*R*,12*R*,17*S*,19*R*-**5** (Fig. 6B). Thus, the structure including absolute configuration of **5** was determined and named heronamide K.

Heronamide L (**6**) was purified as a white powder owning a molecular formula of $C_{27}H_{41}NO_7$ (eight degrees of unsaturation) as presented by the HRESIMS peak at m/z 492.2976 [M + H]$^+$. The ^{1}H NMR, ^{13}C NMR, and HSQC spectra in DMSO-d_6 (Table 2) revealed the presence of one amide carbonyl (δ_C 175.1), one nonprotonated olefinic carbon (δ_C 136.7), and three olefinic methines ($\delta_{C/H}$ 133.7/5.48, 133.1/5.38, and 126.6/5.35), satisfying three out of eight degrees of unsaturation. Therefore, **6** should have a pentacyclic skeleton to explain the remaining five degrees of unsaturation. Detailed analysis of ^{1}H–^{1}H COSY correlations provided substructures as shown in Fig. 7A. HMBC correlations from 3-OH to C-2, C-3, C-4, from H_3-26 to C-5, C-6, C-7, from H_3-27 to C-13, C-14, C-15, and from NH to C-1, C-2 further helped determine the planar structure of **6**. The relative configuration of **6** was deduced by careful interpretation of the NOESY experiment (Fig. 7B). Despite the lack of a calculated ECD result, the absolute configuration of **6** could be determined

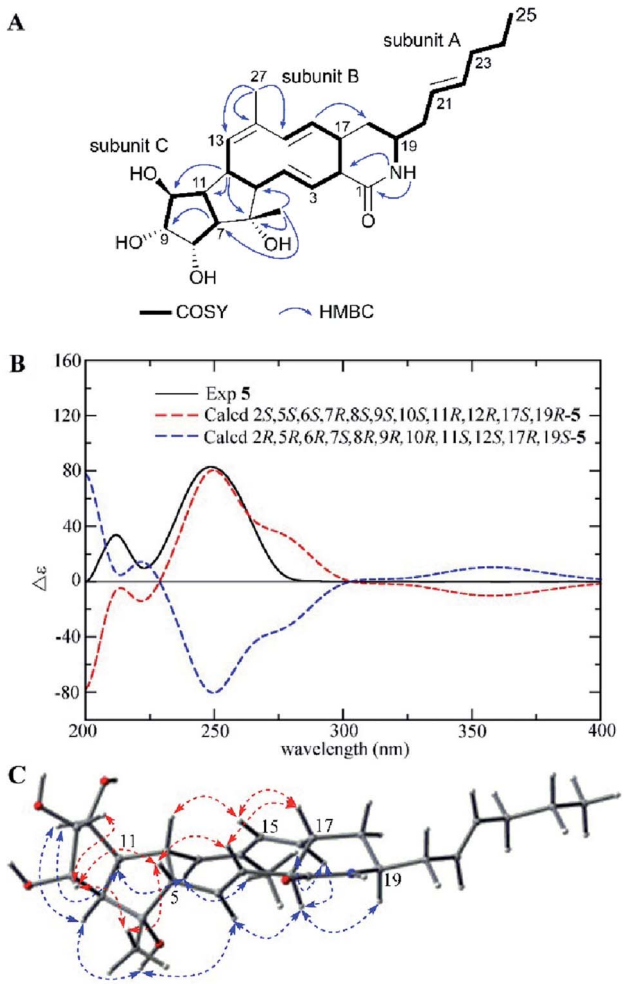

Fig. 6 (A) COSY and key HMBC correlations of **5**, (B) comparison of the experimental ECD spectra of **5** with the calculated ECD spectra, and (C) key NOEs observed in **5**.

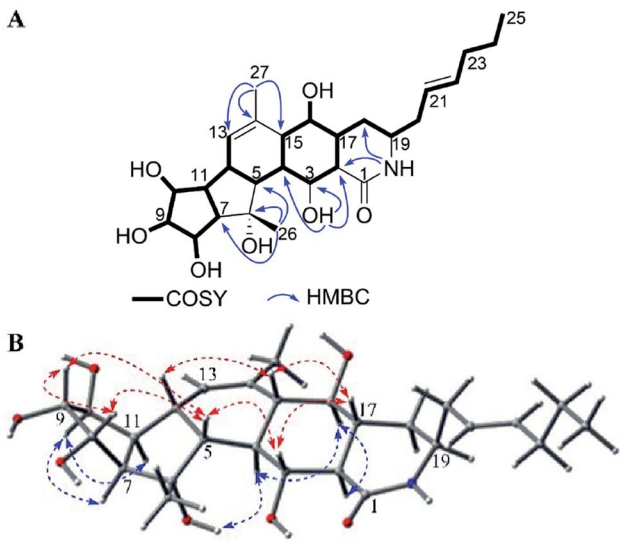

Fig. 7 (A) COSY and key HMBC correlations of **6**. (B) Key NOE correlations observed in **6**.

by comparing the spectra data with **5** as well as analysis of the possible biosynthetic pathway (Scheme 1), which possessed high stereospecificity and deduced the same configurations of compounds **1–6**. Thereby, the structure of **6** was established as shown.

Niveamide B (**10**) possessed a molecular formula of $C_{16}H_{27}NO_3$ deduced from HRESIMS peak at *m*/*z* 282.2075 $[M + H]^+$. The ^1H NMR, ^{13}C NMR (Table 2) together with HSQC displayed one amide carbonyl carbon (δ_C 167.8), four olefinic methines ($\delta_{C/H}$ 131.4/5.40, 128.7/5.36, 127.9/5.36, and 126.2/5.32), two aliphatic methines ($\delta_{C/H}$ 47.8/3.67, 38.7/2.31), five methylenes ($\delta_{C/H}$ 36.2/2.06; 36.2/1.98; 35.7/2.23, 2.02; 33.5/1.92; and 21.5/1.32), three methyls ($\delta_{C/H}$ 22.1/1.76, 15.8/1.01, and 12.8/0.85). However, because of low sample quantity, the ^{13}C NMR spectrum didn't present the carboxylic carbon signal at δ_C 176.6, which was supported by the HMBC correlations from H-2 (δ_H 2.31) and H_3-14 (δ_H 1.01) to C-1 (δ_C 176.6). The ^1H and ^{13}C NMR observed for **10** closely resembled the known compound niveamide (**11**)[10] except for the presence of $-CH_2CH-$ and the absence of $-CH{=}C-$ moiety. ^1H–^1H COSY correlations between H_3-14/H-2, H-2/H-3, and H-3/H-4 and HMBC correlations from H-2, H_3-14 to C-1 demonstrated the structure of **10** and it was named as niveamide B.

The compound BE-14106 (**8**) and its deoxy analogue GT-32B (**9**) were reported to possess weak antibacterial, antifungal, and moderate cytotoxic activities.[5,12] In 2016, BE-14106 was found to show potent growth inhibition against fission yeast cells with an MIC value of 0.50 μM compared to the clinically used amphotericin B (MIC = 0.27 μM).[7] BE-14106-6 (**7**) was shown to exhibit moderate cytotoxicities.[11] In this report, biological activities including antimicrobial activities against *Bacillus subtilis*, *Staphylococcus aureus*, *Escherichia coli*, *Candida albicans*, and *Candida parapsilosis*; cytotoxicities against BGC-823, H460, Ishikawa, SMMC-7721, and inhibitory effects on lipopolysaccharide-induced NO production in BV2 microglial cells of **1–6** and **8–11** were tested. However, except that compounds **8** and **9** showed weak cytotoxicities at 100 μM, no significant activity was detected for these compounds at 100 μg mL^{-1} for antimicrobial activities or 100 μM for cytotoxicities and NO production inhibitory activity.

Experimental section

General experimental procedures

Optical rotations were obtained using an Anton Paar MCP 200 polarimeter. Ultraviolet spectra were obtained with a Beckman Coulter DU 730 nucleic acid/protein analyzer. CD spectra were measured on a Biologic MOS-450 spectra polarimeter (Biologic Science, Claix, France). IR spectra were performed on a Bruker Tensor 27 FT-IR spectrophotometer (film). NMR spectra were recorded on a Bruker AV-600 spectrometer using tetramethylsilane as an internal standard, and the chemical shifts were recorded in δ values. HRESIMS were measured using a Bruker micro TOF-Q mass instrument (Bruker Daltonics, Billerica, MA, USA). ESIMS were performed on an Agilent 1290-6420 Triple

Quadrupole LC-MS spectrometer. Silica gel (300–400 mesh, and 1200–1500 mesh, Qingdao Marine Chemical Ltd., Qingdao, China), Sephadex LH-20 (GE Healthcare Biosciences AB, Uppsala, Sweden), YMC*GEL ODS-A (S-50 μm, 12 nm) (YMC Co., Ltd., Kyoto, Japan), and MCI gel (CHP-20P, Mitsubishi Chemical Corp., Tokyo, Japan) were utilized for column chromatography. Semipreparative HPLC was performed using a ODS column (250 mm × 10 mm, 5 μm, YMC-ODS-A). Unless otherwise specified, all chemicals and solvents were purchased from Sinopharm Chemical Reagent Co., Ltd. (Shenyang, China). Biological assays were analyzed using a microplate reader (BioTek Synergy H1, BioTek Instruments, Inc., Vermont, USA).

Microbial material

The producing organism was isolated from a forest soil sample collected in Great Khingan Mountains, Northeastern of China in July 2003. The strain was assigned to be *Streptomyces niveus* based on morphological characteristics and 16S rRNA gene sequences. The Blast result showed that the sequence was most similar (99.78%) to the sequence of *S. niveus* (strain: NRRL 2466^T, GenBank accession no. DQ442532). The strain (no. YIM 32862) was deposited in Yunnan Institute of Microbiology, Yunnan University, China.

Fermentation, extraction, and isolation

The strain *S. niveus* was inoculated to a 100 mL seed medium consisting of 4 g L^{-1} yeast extract, 4 g L^{-1} glucose, 5 g L^{-1} malt extract, and 1.0 mL of trace element solution at a pH of 7.2 without adjustment. The flasks were cultivated for 2 days on a rotary shaker (180 rpm) at 28 °C, followed by inoculation to a fermentation medium (10 g L^{-1} soybean meal, 2 g L^{-1} peptone, 20 g L^{-1} glucose, 5 g L^{-1} soluble starch, 2 g L^{-1} yeast extract, 4 g L^{-1} NaCl, 0.5 g L^{-1} K_2HPO_4, 0.5 g L^{-1} $MgSO_4 \cdot 7H_2O$, and 2 g L^{-1} $CaCO_3$, pH = 7.8) with a 10% volume. The fermentation was incubated at 28 °C for 7 days on a rotary shaker at 180 rpm.

The completed fermentation culture (140 L) was centrifuged (4000 rpm, 5 min) into supernatant and mycelium, and the supernatant was extracted by EtOAc four times and evaporated to yield crude extract 60 g. The dried extract was subjected to silica gel (300–400 mesh) column chromatography eluting with a gradient CH_2Cl_2–MeOH solvent system (from 50 : 1 to 10 : 1, and finally 4 : 1) to give seven fractions: Fr. A–G. Fractions A and B were filtrated to obtain compound **9** (100 mg) and compound **8** (35.0 mg), respectively. Fraction C was subjected to a Sephadex LH-20 column (MeOH) to produce nine sub-fractions, Fr. C1–C9. Fr. C3 was put on a silica gel (1200–1500 mesh) for column chromatography (CH_2Cl_2–MeOH, 20 : 1) and further purified by semipreparative HPLC (MeOH–H_2O 65 : 35) to yield **10** (3.9 mg) and **11** (14.7 mg). Fraction F was subjected to Sephadex LH-20 chromatography (MeOH) to produce 2 sub-fractions, Fr. F1 and F2. Sub-fraction F2 was divided into six fractions, F2.1–F2.6 by silica gel (1200–1500 mesh) column chromatography (CH_2Cl_2–MeOH, 8 : 1). Sub-fraction F2.4 was further put on silica gel (1200–1500 mesh) eluting with CH_2Cl_2–acetone (1 : 1) followed by semipreparative HPLC (MeOH–H_2O 55 : 45) to yield **1** (22.0 mg), **7** (20.0 mg). Sub-fraction F2.5 was subjected to silica gel (1200–1500 mesh) column chromatography (CH_2Cl_2–acetone, 1 : 1) and further purified by semipreparative HPLC (MeOH–H_2O 65 : 35) to give **2** (5.6 mg). Fraction G was subjected to a MCI gel CHP-20P column and eluted with MeOH to produce 6 sub-fractions, Fr. G1–G6. Fr. G2–G5 was subjected to silica gel (1200–1500 mesh) column chromatography (CH_2Cl_2–MeOH, 6 : 1 or 8 : 1) separately and further separated by semipreparative HPLC (MeOH–H_2O 65 : 35 or 60 : 40) to afford **6** (5.0 mg), **3** (4.5 mg), **4** (2.0 mg), and **5** (9.4 mg), respectively.

Heronamide G (1). Colorless solid; $[\alpha]_D^{20}$ −48 (*c* 0.10, MeOH); UV_{max} (MeOH) λ_{max} (log ε) 253 (4.31), 217 (4.73) nm; IR (film) ν_{max} 3351, 3023, 2962, 2924, 1667, 1433, 1377, 1102, 1074, and 974 cm^{-1}; CD (0.5 mg mL^{-1}, MeOH) λ_{max} ($\Delta\varepsilon$) 210 (85.22), 256 (−105.99); ^1H NMR and ^{13}C NMR data, see Table 1; ESIMS *m*/*z* 456 $[M + H]^+$, 478 $[M + Na]^+$; HRESIMS *m*/*z* 456.2758 $[M + H]^+$ (calcd for $C_{27}H_{38}NO_5$, 456.2750).

Heronamide H (2). White powder; $[\alpha]_D^{20}$ +48 (*c* 0.10, MeOH); UV_{max} (MeOH) λ_{max} (log ε) 268 (4.50), 222 (5.19) nm; IR (film) ν_{max} 3379, 2958, 2923, 1678, 1405, 1369, 1102, 1047, and 969 cm^{-1}; CD (0.9 mg mL^{-1}, MeOH) λ_{max} ($\Delta\varepsilon$) 229 (−18.39), 239 (22.10), and 266 (−229.20); ^1H NMR and ^{13}C NMR data, see Table 1; ESIMS *m*/*z* 474 $[M + H]^+$, 496 $[M + Na]^+$; HRESIMS *m*/*z* 474.2861 $[M + H]^+$ (calcd for $C_{27}H_{40}NO_6$, 474.2856).

Heronamide I (3). White powder; $[\alpha]_D^{20}$ +280 (*c* 0.08, MeOH); UV (MeOH) λ_{max} (log ε) 230 (5.20) nm; IR (film) ν_{max} 3361, 2957, 2928, 1598, 1411, 1286, 1071, and 974 cm^{-1}; CD (1.25 mg mL^{-1}, MeOH) λ_{max} ($\Delta\varepsilon$) 247 (−42.88), 274 (141.07); ^1H NMR and ^{13}C NMR data, see Table 1; ESIMS *m*/*z* 474 $[M + H]^+$, 496 $[M + Na]^+$; HRESIMS *m*/*z* 474.2870 $[M + H]^+$ (calcd for $C_{27}H_{40}NO_6$, 474.2856).

Heronamide J (4). White powder; $[\alpha]_D^{20}$ −20 (*c* 0.10, MeOH); UV (MeOH) λ_{max} (log ε) 225 (4.68) nm; IR (film) ν_{max} 3351, 2958, 2924, 1658, 1596, 1421, 1072, and 972 cm^{-1}; CD (0.6 mg mL^{-1}, MeOH) λ_{max} ($\Delta\varepsilon$) 218 (−42.13), 253 (52.73); ^1H NMR and ^{13}C NMR data, see Table 1; ESIMS *m*/*z* 474 $[M + H]^+$, 496 $[M + Na]^+$; HRESIMS *m*/*z* 474.2869 $[M + H]^+$ (calcd for $C_{27}H_{40}NO_6$, 474.2856).

Heronamide K (5). White powder; $[\alpha]_D^{20}$ −40 (*c* 0.10, MeOH); UV (MeOH) λ_{max} (log ε) 247 (4.47), 204 (5.00) nm; IR (film) ν_{max} 3382, 2958, 2928, 1651, 1435, 1332, 1111, 1079, 975 cm^{-1}; CD (0.5 mg mL^{-1}, MeOH) λ_{max} ($\Delta\varepsilon$) 212 (33.91), 249 (82.86); ^1H NMR and ^{13}C NMR data, see Table 2; ESIMS *m*/*z* 458 $[M + H]^+$, 480 $[M + Na]^+$; HRESIMS *m*/*z* 458.2912 $[M + H]^+$ (calcd for $C_{27}H_{40}NO_5$, 458.2906).

Heronamide L (6). White powder; $[\alpha]_D^{20}$ −24 (*c* 0.10, MeOH); IR (film) ν_{max} 3368, 2956, 2928, 1636, 1415, 1337, 1114, 1022, and 974 cm^{-1}; ^1H NMR and ^{13}C NMR data, see Table 2; ESIMS *m*/*z* 492 $[M + H]^+$; HRESIMS *m*/*z* 492.2976 $[M + H]^+$ (calcd for $C_{27}H_{42}NO_7$, 492.2961).

Niveamide B (10). Colorless solid; $[\alpha]_D^{20}$ −20 (*c* 0.08, MeOH); IR (film) ν_{max} 2959, 2928, 2872, 1709, 1648, 1554, 1435, 1377, and 970 cm^{-1}; ^1H NMR and ^{13}C NMR data, see Table 2; ESIMS *m*/*z* 282 $[M + H]^+$; HRESIMS *m*/*z* 282.2075 $[M + H]^+$ (calcd for $C_{16}H_{28}NO_3$, 282.2069).

ECD calculations

The conformational search was performed by CONFLEX,[13,14] based on molecular mechanics with MMFF94S force fields. Selected conformers whose energies were 3 kcal mol^{-1} higher than the conformer with the lowest energy were further optimized by the density functional theory method at the B3LYP/6-31G (d) level in Gaussian 09 program package,[15] which was further checked by frequency calculation and resulted in no imaginary frequencies. The ECDs of the conformers of **1–5** were then calculated by the TDDFT method at B3LYP/6-311 ++ G (2d, p) level with the CPCM model in methanol solution. The final ECD curves were generated based on the rotatory strengths by SpecDis[16] and calculated from the spectra of individual conformers according to their contribution to the Boltzmann weighting. The theoretical spectra have been corrected based on the UV correction.

Antimicrobial assay

A micro broth dilution assay was used to evaluate the antimicrobial activity of **1–6** and **8–11** against *Bacillus subtilis* ATCC 6633, *Staphylococcus aureus* ATCC 25923, *Escherichia coli* ATCC 25922, *Candida albicans* ATCC MYA-2876, and *Candida parapsilosis* ATCC 22019 as previously reported.[17] Ciprofloxacin and amphotericin B were used as positive controls against bacteria and fungi, respectively.

Cytotoxicity assay

The human gastric carcinoma cell line (BGC-823), human large-cell lung carcinoma cell line (H460), human endometrial carcinoma cell line (Ishikawa), and human hepatocellular carcinoma cell line (SMMC-7721) were used to evaluate the cytotoxic effects of compounds **1–6** and **8–11** using the MTT method as previously reported.[17] Adriamycin was assayed as a positive control.

Inhibition of NO production assay

The inhibitory effects on lipopolysaccharide-induced NO production in BV2 microglial cells was measured using the Griess reaction to indicate NO production and examined according to a previously described protocol.[18,19] The cell culture and data analysis of NO production inhibition followed a previously published method.[20] Dexamethasone was used as the positive control.

Conclusions

In summary, we isolated and characterized six new polyene macrolactams, heronamides G–L (**1–6**), one new polyenoic acid derivative, niveamide B (**10**), and four known compounds, BE-14106-6 (**7**), BE-14106 (**8**), GT32-B (**9**), and niveamide (**11**), from the fermentation broth of *Streptomyces niveus*. The absolute configurations of compounds **1–6** were determined by calculated ECD spectra and analysis of the possible biosynthetic pathways. However, compounds **1–6** and **8–11** did not exhibit any significant antimicrobial activities, cytotoxicities, or inhibitory effects on lipopolysaccharide-induced NO production in BV2 microglial cells.

Conflicts of interest

There are no conflicts to declare.

Acknowledgements

This work was funded by National Natural Science Foundation of China (No. 81573327, 31460005, and 81771167) and the Fundamental Research Funds for the Central Universities, China (No. N172004004 and N172008008).

Notes and references

1 K. Fujita, R. Sugiyama, S. Nishimura, N. Ishikawa, M. A. Arai, M. Ishibashi and H. Kakeya, *J. Nat. Prod.*, 2016, **79**, 1877–1880.
2 T. J. Booth, S. Alt, R. J. Capon and B. Wilkinson, *Chem. Commun.*, 2016, **52**, 6383–6386.
3 P. Yu, A. Patel and K. N. Houk, *J. Am. Chem. Soc.*, 2015, **137**, 13518–31523.
4 K. Katsuhisa, N. Shigeru, S. Hajime, K. Hisao and S. Hiroyuki, *J. Antibiot.*, 1992, **45**, 868–874.
5 T. Isami, O. Yashushi, N. Yashushi, O. Keiko and M. Tamio, *J. Antibiot.*, 1997, **50**, 186–188.
6 H. Jorgensen, K. F. Degnes, A. Dikiy, E. Fjaervik, G. Klinkenberg and S. B. Zotchev, *Appl. Environ. Microbiol.*, 2010, **76**, 283–293.
7 R. Raju, A. M. Piggott, M. M. Conte and R. J. Capon, *Org. Biomol. Chem.*, 2010, **8**, 4682–4689.
8 W. Zhang, S. Li, Y. Zhu, Y. Chen, Y. Chen, H. Zhang, G. Zhang, X. Tian, Y. Pan, S. Zhang, W. Zhang and C. Zhang, *J. Nat. Prod.*, 2014, **77**, 388–391.
9 R. Sugiyama, S. Nishimura, N. Matsumori, Y. Tsunematsu, A. Hattori and H. Kakeya, *J. Am. Chem. Soc.*, 2014, **136**, 5209–5212.
10 Y. Zhu, W. Zhang, Y. Chen, C. Yuan, H. Zhang, G. Zhang, L. Ma, Q. Zhang, X. Tian, S. Zhang and C. Zhang, *ChemBioChem*, 2015, **16**, 2086–2093.
11 L. Li, Y. Cai, Y. Jiang, J. Liu, J. Ma, C. Yuan, Y. Mu, L. Han and X. Huang, *Bioorg. Med. Chem. Lett.*, 2016, **26**, 1599–1604.
12 H. Jørgensen, K. F. Degnes, H. Sletta, E. Fjaervik, A. Dikiy, L. Herfindal, P. Bruheim, G. Klinkenberg, H. Bredholt, G. Nyga, S. O. Døskeland, T. E. Ellingsen and S. B. Zotchev, *Chem. Biol.*, 2009, **16**, 1109–1121.
13 H. Goto and E. Osawa, *J. Am. Chem. Soc.*, 1989, **111**, 8950–8951.
14 H. Goo and E. Osawa, *J. Chem. Soc., Perkin Trans. 2*, 1993, 187–198.
15 G. Mazeo, E. Santoro, A. Andolfi, A. Cimmino, P. Troselj, A. G. Petrovic, S. Superchi, A. Evidente and N. Berova, *J. Nat. Prod.*, 2013, **76**, 588–599.
16 T. Bruhn, A. Schaumloeffel, Y. Hemberger and G. Bringmann, *Chirality*, 2013, **25**, 243–249.

17 Q. Ma, L. Han, X. Bi, X. Wang, Y. Mu, P. Guan, L. Li and X. Huang, *Phytochemistry*, 2016, **131**, 150–157.
18 R. A. Hunter, W. L. Storm, P. N. Coneski and M. H. Schoenfisch, *Anal. Chem.*, 2013, **85**, 1957–1963.
19 Z. Li, Z. Li, J. Bai, D. Meng, N. Li, Y. Pei, F. Zhao and H. Hua, *J. Nat. Prod.*, 2014, **25**, 792–799.
20 J. Xu, C. Yuan, G. Wang, J. Luo, H. Ma, L. Xu, Y. Mu, Y. Li, N. Seeram, X. Huang and L. Li, *J. Agric. Food Chem.*, 2018, **66**, 571–580.